DALTON

Dinuclear alkoxide-bridged ruthenium(II) complexes with Class III mixed-valence states: a structural and spectroelectrochemical study †

David A. Bardwell,[a] Lockhart Horsburgh,[b] John C. Jeffery,[a] Laurent F. Joulié,[a] Michael D. Ward,*[,a] Ian Webster[a] and Lesley J. Yellowlees[b]

[a] *School of Chemistry, University of Bristol, Cantock's Close, Bristol BS8 1TS, UK*
[b] *Department of Chemistry, University of Edinburgh, The King's Buildings, West Mains Road, Edinburgh EH9 3JJ, UK*

Reaction of $[Ru(bipy)_2Cl_2]$ (bipy = 2,2′-bipyridine) with NaOMe or KOH in methanol at reflux afforded high yields of the dinuclear complex $[\{Ru(bipy)_2\}_2(\mu\text{-}OMe)_2][PF_6]_2$ **1**. Reaction of **1** with NaOEt in ethanol resulted in exchange of the bridge to give $[\{Ru(bipy)_2\}_2(\mu\text{-}OEt)_2][PF_6]_2$ **2**. The crystal structures of **1** and **2** showed that the complex cations have similar structures in which two $Ru(bipy)_2^{2+}$ fragments, which for steric reasons have the same absolute configuration, are linked by two alkoxide bridges. Each dinuclear complex cation is therefore chiral, and there are equal numbers of each enantiomer in the crystals of both **1** and **2**. Electrochemical measurements showed that there is a strong electrochemical interaction between the metal centres, with separations of 0.55 and 0.57 V respectively between the two Ru^{II}–Ru^{III} couples corresponding to K_c values of 3×10^9 and 6×10^9 for the mixed-valence states of **1** and **2**. A spectroelectrochemical study of complex **1** showed that oxidation of the mixed-valence state results in a new transition in the electronic spectrum at *ca.* 1800 nm with $\varepsilon = 5000$ dm^3 mol^{-1} cm^{-1}, which disappears on further oxidation to the Ru^{III} state. The observations that this transition is not solvatochromic, and that the half-width of the peak is much narrower than the value predicted by Hush theory for vectorial intervalence charge-transfer bands, both point to a class III (fully delocalised) mixed-valence state; delocalisation between the d_π orbitals of the two metal centres is facilitated by good overlap with oxygen p_π orbitals in the Ru_2O_2 core. The magnitude of the electronic interaction V_{ab} is estimated to be 2800 cm^{-1}, similar in magnitude to that of the Creutz–Taube ion.

Polynuclear complexes containing polypyridylruthenium(II) fragments are of particular interest for the study of mixed valency because of their kinetic inertness in both the +II and +III oxidation states, generally reversible electrochemical behaviour, and good π-donor ability which allows interaction with bridging ligand orbitals.[1] Mixed-valence complexes provide an ideal way of studying the most fundamental process in chemistry, electron transfer, under controlled conditions, and for this reason the preparation and characterisation of complexes which exhibit isolable mixed-valence states continues to be an important goal in synthetic co-ordination chemistry.[2,3]

We describe in this paper the syntheses, crystal structures, and electrochemical and spectroscopic properties of some dinuclear ruthenium complexes in which the metal centres are linked by alkoxide ligands. The strong interaction between the metal atoms as a result of the single-atom bridge and the short metal–metal separations results in well defined mixed-valence states. A preliminary communication on part of this work has been published.[4]

Experimental

General procedures and the intrumentation used for routine spectroscopic analyses,[5] and for the spectroelectrochemical studies,[6] have been described elsewhere. Syntheses of the complexes, and chacterisation data, are given in the earlier communication.[4]

X-Ray crystallography

The determination of the crystal structure of $[\{Ru(bipy)_2\}_2(\mu\text{-}OEt)_2][PF_6]_2\cdot 2MeCN\cdot Et_2O$ (**2**·2MeCN·Et$_2$O) (bipy = 2,2′-bipyridine) was described in the preliminary communication.[4] The complex $[\{Ru(bipy)_2\}_2(\mu\text{-}OMe)_2][PF_6]_2\cdot 0.33NH_4PF_6\cdot Et_2O$ (**1**·0.33NH_4PF_6·Et$_2$O) was recrystallised by diffusion of ether vapour into concentrated MeCN solutions, to give black blocks. A crystal of dimensions 0.5 × 0.2 × 0.2 mm was transferred rapidly from the mother-liquor to a stream of cold N_2 (173 K) on the diffractometer; data were collected at this temperature using a Siemens SMART three-circle diffractometer with a CCD area detector. Graphite-monochromatised Mo-Kα X-radiation ($\bar{\lambda} = 0.710\,73$ Å) was used.

Crystal data. $C_{46}H_{48}F_{14}N_{8.33}O_3P_{2.33}Ru$, $M = 1306.0$, trigonal, space group $R\bar{3}c$, $a = 37.148(4)$, $b = 37.148(4)$, $c = 39.120(5)$ Å, $U = 46\,751(9)$ Å^3, $Z = 36$, $D_c = 1.670$ g cm^{-3}, μ(Mo-Kα) = 0.753 mm^{-1}, $F(000) = 23\,592$.

68 590 Reflections were collected to $2\theta_{max} = 50°$; after merging, these gave 9205 independent reflections with $R_{int} = 0.04$. Data were corrected for Lorentz, polarisation and absorption effects, the latter using an empirical method based on multiple measurements of equivalent data.

The structure was solved by conventional direct methods using SHELXTL and refined by full-matrix least squares on all F^2 data with the SHELXTL 5.03 package using a Silicon Graphics Indigo R4000 computer.[8] All non-hydrogen atoms were refined anisotropically; hydrogen atoms were included in calculated positions and refined with isotropic thermal parameters. Refinement of 688 parameters with 32 restraints converged at $wR_2 = 0.200$ ($R_1 = 0.063$). The largest residual peak and hole were +1.256 and −1.343 e Å^{-3}.

Atomic coordinates, thermal parameters and bond lengths and angles have been deposited at the Cambridge Crystallographic Data Centre (CCDC). See Instructions for Authors, *J. Chem. Soc., Dalton Trans.*, 1996, Issue 1. Any request to the

† *Non-SI unit employed:* eV ≈ 1.60 × 10^{-19} J.

CCDC for this material should quote the full literature citation and the reference number 186/72.

Results and Discussion

Syntheses of complexes

The preparation and study of the alkoxide-bridged dinuclear complexes $[\{Ru(bipy)_2\}_2(\mu\text{-}OR)][PF_6]_2$ (R = Me **1** or Et **2**) arose from the observation of trace amounts of a purple by-product whenever we prepared complexes using $[Ru(bipy)_2Cl_2]$ in MeOH, especially under basic conditions. Chromatographic isolation of the by-product allowed it to be tentatively identified as **1** by FAB mass spectrometry, and realising that this was an unknown and interesting material we sought to prepare it in larger quantities. Simple reflux of $[Ru(bipy)_2Cl_2]$ in MeOH to which NaOMe or KOH was added gave **1** in high yield. In contrast, reaction of $[Ru(bipy)_2Cl_2]$ with NaOEt in refluxing ethanol gave very poor yields of **2**; however, alkoxide exchange could be effected readily by treating **1** with refluxing NaOEt–EtOH.[4] Both complexes are a beautiful inky purple in solution, and effectively black as solids. Their formulation was made on the basis of elemental analyses and FAB mass spectra. The ^1H NMR spectra of the complexes are identical in the aromatic region and show the expected eight resonances that are entirely typical of $Ru^{II}(bipy)_2X_2$ groups. The protons from the alkoxide substituents are slightly shielded due to their proximity to the aromatic ring currents of the bipy ligands: for the methyl groups of **1**, in MeCN, δ 2.25; for **2**, the CH_2 and CH_3 protons resonate at δ 2.70 and 0.01 respectively.

Complexes **1** and **2** are the first examples of alkoxide-bridged dinuclear ruthenium(II) complexes. Oxo-bridged ruthenium(III) complexes of the type $[\{Ru(bipy)_2X\}(\mu\text{-}O)]^{n+}$ (X = Cl or NO_2, n = 2; X = H_2O, n = 4) are known and permit access to ruthenium(III,IV) mixed-valence states.[9] The closest analogue to **1** and **2** is the chloride-bridged dinuclear complex $[\{Ru^{II}(bipy)_2\}_2(\mu\text{-}Cl)_2]^{2+}$ which was reported by Meyer and co-workers[10] in 1978. In passing it is worth pointing out that complex **1** was almost certainly prepared by Meyer's group in 1979; they reported that reaction of $[Ru(bipy)_2(dme)]^{2+}$ (dme = 1,2-dimethoxyethane) with NaOMe–MeOH afforded a purple complex which was assumed to be $[Ru(bipy)_2(OMe)_2]$ but was not isolated from solution. It is likely that this was in fact the dication of **1**, especially in view of the similarity of its electronic spectrum to that of **1**.[11]

Structures of complexes 1 and 2

The crystal structure of complex **1** is shown in Fig. 1. That of **2** was described in the preliminary communication, and is recalled in Fig. 2 for comparison: it will be discussed first as it is simpler. Each dinuclear cation of **2** has approximate (non-crystallographic) C_2 symmetry and is therefore optically active, with both ruthenium centres having the same configuration. If the ethyl groups of the alkoxide bridges are ignored, the symmetry of the $\{Ru(bipy)_2\}_2(\mu\text{-}O)_2$ complex core is D_2; the fact that the ethyl groups do not lie in the Ru_2O_2 plane reduces the symmetry to C_2. The core structure is similar to that of $[\{Mn(bipy)_2\}_2(\mu\text{-}O)_2]^{3+}$.[12] The crystal is racemic, with opposite enantiomers related by a crystallographic inversion centre. Overlap of near-parallel sections of bipy ligands on the different metal centres results in aromatic π-stacking interactions, with average separations of 3.3 Å between the overlapping segments (ring 4 overlaps with 8, and ring 2 with 6, according to the numbering scheme used). The *meso* diastereoisomer, in which the two chiral centres would be opposite, is sterically impossible due to the closeness of the two chiral centres, and would require pairs of bipy ligands to occupy the same region of space.

The bond lengths around the ruthenium centres are typical.[4] The Ru–O bond distances lie between 2.097(7) and 2.114(7) Å and are therefore essentially identical within the limits of error of the determination, and are similar to Ru^{II}–O (phenolate) bond lengths.[13] The Ru–N bond distances split into two sets: for the N atoms *trans* to the alkoxides they average 2.035 Å, whereas for the N atoms *trans* to other pyridine rings the average distance is slightly longer at 2.057 Å, which is the same as in $[Ru(bipy)_3]^{2+}$.[14] A slight *trans* effect is therefore in evidence, with the d_π–p_π back bonding between ruthenium and the pyridyl rings being strengthened along axes which also contain electron-donor alkoxide ligands.

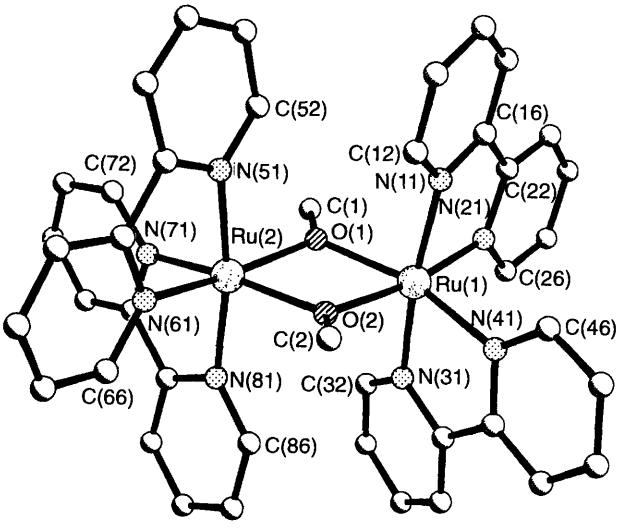

Fig. 1 Crystal structure of the cation in complex **1**

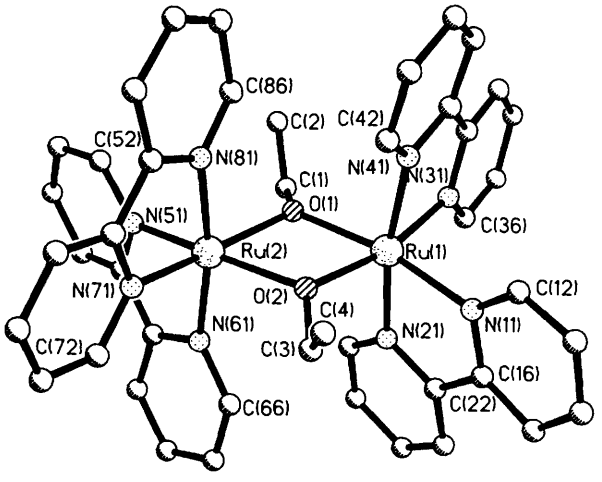

Fig. 2 Crystal structure of the cation in complex **2**

The structure of complex **1** is complicated by the fact that it has cocrystallised with some of the NH_4PF_6 that was used to precipitate the complex and had evidently not been completely washed out of the batch of crude material that was used to prepare the crystals. The crystal contains one equivalent of NH_4PF_6 per three molecules of **1**, with the ammonium cation and the extra hexafluorophosphate anion disordered about a three-fold axis. The structural parameters for the complex dication, however, are as expected (Table 1) and are similar to those of **2**.[4] The Ru–O bond distances lie between 2.087(4) and 2.105(4) Å, and the Ru–N bond distances are split into two groups, with an average value of 2.023 Å for the bonds *trans* to the alkoxide donors and 2.048 Å for the bonds *trans* to other pyridine rings. The Ru · · · Ru distance is 3.316 Å, very similar to that of **2**. Although each complex dication is optically active, the crystal contains equal numbers of each enantiomer and is therefore racemic.

There are two minor differences between the structures of the

Table 1 Selected bond lengths (Å) and angles (°) for the cation of complex **1**

Ru(1)–N(21)	2.025(5)	Ru(2)–N(61)	2.017(6)
Ru(1)–N(41)	2.023(5)	Ru(2)–N(71)	2.026(5)
Ru(1)–N(31)	2.050(5)	Ru(2)–N(51)	2.040(6)
Ru(1)–N(11)	2.053(5)	Ru(2)–N(81)	2.048(5)
Ru(1)–O(1)	2.104(4)	Ru(2)–O(2)	2.087(4)
Ru(1)–O(2)	2.105(4)	Ru(2)–O(1)	2.090(4)
N(21)–Ru(1)–N(41)	95.2(2)	N(61)–Ru(2)–N(71)	90.8(2)
N(21)–Ru(1)–N(31)	94.3(2)	N(61)–Ru(2)–N(51)	79.6(3)
N(41)–Ru(1)–N(31)	79.4(2)	N(71)–Ru(2)–N(51)	95.1(2)
N(21)–Ru(1)–N(11)	79.2(2)	N(61)–Ru(2)–N(81)	93.1(2)
N(41)–Ru(1)–N(11)	97.6(2)	N(71)–Ru(2)–N(81)	79.2(2)
N(31)–Ru(1)–N(11)	172.7(2)	N(51)–Ru(2)–N(81)	170.7(2)
N(21)–Ru(1)–O(1)	98.0(2)	N(61)–Ru(2)–O(2)	97.6(2)
N(41)–Ru(1)–O(1)	165.0(2)	N(71)–Ru(2)–O(2)	168.0(2)
N(31)–Ru(1)–O(1)	92.3(2)	N(51)–Ru(2)–O(2)	94.9(2)
N(11)–Ru(1)–O(1)	92.0(2)	N(81)–Ru(2)–O(2)	91.6(2)
N(21)–Ru(1)–O(2)	170.3(2)	N(61)–Ru(2)–O(1)	167.6(2)
N(41)–Ru(1)–O(2)	92.8(2)	N(71)–Ru(2)–O(1)	97.6(2)
N(31)–Ru(1)–O(2)	92.6(2)	N(51)–Ru(2)–O(1)	90.6(2)
N(11)–Ru(1)–O(2)	94.2(2)	N(81)–Ru(2)–O(1)	97.4(2)
O(1)–Ru(1)–O(2)	74.9(2)	O(2)–Ru(2)–O(1)	75.6(2)
C(2)–O(2)–Ru(1)	129.9(4)	C(2)–O(2)–Ru(2)	124.0(4)
C(1)–O(1)–Ru(1)	128.1(4)	C(1)–O(1)–Ru(2)	126.3(4)
Ru(2)–O(1)–Ru(1)	104.5(2)	Ru(2)–O(2)–Ru(1)	104.6(2)

cations of complexes **1** and **2**. First, the coordination-sphere bond lengths for **1** are all fractionally shorter than in **2** by about 0.01 Å. This is at about the limit of significance, and may be ascribed either to different crystal-packing effects or to the slightly greater steric influence of the ethyl groups of **2** compared to the methyl groups of **1**. Secondly, since the methoxide ligands of **1** lie in the Ru_2O_2 plane, the complex cation has (non-crystallographic) D_2 symmetry.

Molecular orbitals of complex 1

A simple frontier molecular orbital (MO) diagram for complexes **1** and **2** is given in Fig. 3. The z axis is taken to be the Ru–Ru axis, and the x axis is perpendicular to the Ru_2O_2 plane. Assuming local D_{2h} symmetry (*i.e.* ignoring the sense of attachment of the chelate linkages), then the two d_{xz} orbitals give b_{3u} and b_{2g} combinations; the two d_{xy} orbitals give b_{1g} and a_u combinations and the two d_{z^2} orbitals give a_g and b_{1u} combinations.† The oxygen p_x orbitals give b_{3u} (symmetric) and b_{1g} (antisymmetric) combinations. Overlap of the $b_{3u}(p_x)$ and $b_{3u}(d_{xz})$ combinations therefore gives Ru–O bonding and antibonding levels, overlap of the $b_{1g}(p_x)$ and $b_{1g}(d_{xy})$ combinations does the same, and the remaining combinations are non-bonding, assuming no direct metal–metal interaction. This MO diagram is in accord with what would be expected as a consequence of the two π-donor ligands, with, formally, one d_π orbital of each metal centre raised in energy and becoming weakly antibonding.

Complications to this simple picture will arise from deviations from ideal D_{2h} symmetry, from π bonding between the metals and the pyridyl rings and, most importantly, from the possibility of direct overlap between ruthenium d orbitals. Strong Ru–Ru bonds typically require a metal–metal distance

† Use of d_{xz}, d_{xy} and d_{z^2} orbitals in the basis set arises from the choice of axes, which is dictated by the convention used in group-symmetry calculations that the principal axis (here the Ru–Ru axis) is the z axis. Thus the y and z axes lie between the bonds, rather than along them as is more usual: effectively the yz plane is rotated by 45° with respect to the more conventional frame of reference. Consequently the d_{xy} orbital is now one of the two d(σ*) orbitals, and the d_{z^2} orbital is directed between the bond axes rather than along them. If the axes are relabelled so that they are coincident with bonds the end result is of course the same, although more cumbersome to express.

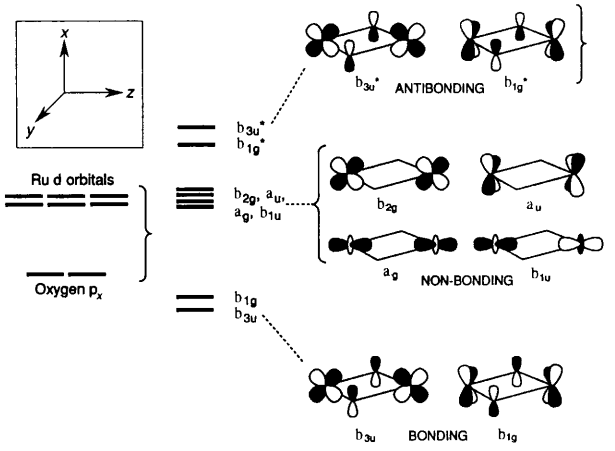

Fig. 3 Symmetries of the frontier molecular orbitals of complexes **1** and **2**

of 2.2–2.4 Å,[15] so the separation of 3.32 Å in **1** and **2** precludes significant Ru–Ru bonding. However, it is still feasible for there to be a weak interaction, so that for example the formally non-bonding $b_{2g}(d_{xz})$ orbital would be weakly π antibonding, the $a_u(d_{xy})$ orbital weakly δ antibonding, and the $a_g(d_{z^2})$ and $b_{1u}(d_{z^2})$ orbitals weakly σ-bonding and -antibonding respectively. The effect would be to split the non-bonding levels, resulting in a wider spread of energies for the formally non-bonding d orbitals than that shown in Fig. 3. The energies of the six highest occupied orbitals were calculated by the ZINDO method‡ to be −11.46, −11.58, −11.74, −11.90, −11.92 and −12.62 eV, confirming that a wide spread of energies does indeed occur and that there is no obvious gap between the four 'non-bonding' and two Ru–O antibonding orbitals.

The composition of the highest occupied molecular orbital (HOMO) was also examined by means of the ZINDO calculation. It is essentially as drawn in Fig. 3, being the b_{3u}* Ru–O π-antibonding level. Its coefficients are 0.28 for each $Ru(d_{xz})$ orbital and 0.12 for each $O(p_x)$ orbital; thus the $Ru_2(\mu\text{-}O)_2$ bridging system accounts for 80% of the HOMO density, with the rest being delocalised over the bipy ligands. This is the orbital which will contain the single electron in the mixed-valence form of the complex, and it seems that the substantial contribution of the oxygen p_x orbitals to the HOMO can provide a good route for delocalisation of the odd electron between the metal centres.

Electrochemical properties of the complexes

Complexes **1** and **2** have essentially identical electrochemical properties (Table 2); a picture of the cyclic and square-wave voltammograms of **2** in MeCN is given in ref. 4. There are two reversible, one-electron oxidations, which are assigned to successive metal-based oxidations to give the $Ru^{II}Ru^{III}$ and Ru^{III}_2 (hereafter denoted [2,3] and [3,3]) species respectively. For both waves the cathodic and anodic peaks are of equal intensity and separated by 70–80 mV independent of scan rate. The separations of 0.55 and 0.57 V between the metal-centred redox couples for **1** and **2** give comproportionation constants (K_c) of 3×10^9 and 6×10^9 respectively, which are of a magnitude characteristic of fully delocalised mixed-valence species (class III according to the Robin and Day

‡ The calculations were performed on a CAChe workstation (CAChe Scientific, Beaverton, OR) using the program supplied (written by M. C. Zerner) with the INDO/1 parameters. The molecule was first constructed using the Editor, and then energy-minimised using the molecular mechanics package with MM2 parameters. The resulting energy-minimised structures were in excellent agreement with the crystal structures (*e.g.* atom–atom separations within 2%) and were then used for the molecular orbital calculations.

Table 2 Electrochemical data for complexes **1** and **2** in MeCN

Complex	$E_{\frac{1}{2}}$/V Ru^{II}–Ru^{I}	Ru^{II}–Ru^{I}	$\Delta E_{\frac{1}{2}}$/V	$E_{\frac{1}{2}}$/V for ligand-based couples
1	−0.09	+0.46	0.55	−1.95, −2.01, −2.29, −2.42
2	−0.06	+0.51	0.57	−1.93, −2.00, −2.31, −2.43

classification).[16] These new complexes are therefore amongst the most strongly electrochemically interacting binuclear ruthenium(II) complexes known. By comparison $K_c = 10^6$ for the Creutz–Taube ion:[17] complexes with significantly higher K_c values than those of **1** and **2** include dinuclear $\{Ru(NH_3)_5\}^{2+}$ complexes with cyanogen,[18] $[N{\equiv}C{-}CR{-}C{\equiv}N]^{-}$[19] or *p*-benzoquinone diimine[20] as bridging ligands, and a complex of a conjugated bis(macrocyclic) ligand.[21] Both **1** and **2** also undergo four reductions at high negative potentials, corresponding to sequential reductions of the four bipyridyl ligands. Although the reduction waves occur in overlapping pairs in the cyclic voltammogram, the $E_{\frac{1}{2}}$ values could be determined by square-wave voltammetry.[4]

Controlled-potential oxidation of a bulk sample of complex **1** in MeCN at +0.2 V *vs.* ferrocene–ferrocenium confirmed the one-electron nature of the first oxidation process ($n = 0.97$ was the experimental value). Although the resulting mixed-valent [2,3] species is stable on the cyclic voltammetric time-scale as shown by the reversibility of the voltammetric wave, the electrochemically generated sample, however, rapidly decomposed to give $[Ru(bipy)_2(NCMe)_2]^{2+}$ (identified by its characteristic absorption maximum at 426 nm),[22] following cleavage of the dinuclear species and replacement of the methoxide ligands by solvent. Very similar electrochemical behaviour is shown by $[\{Ru(bipy)_2\}_2(\mu\text{-}Cl)_2]^{2+}$,[10] which undergoes two successive one-electron Ru^{II}–Ru^{III} couples separated by 0.55 V and slowly decomposes to mononuclear solvated species following oxidation to the mixed-valence state.

Electronic spectra and mixed-valence behaviour of complexes 1 and 2

The electronic spectra of the complexes in their various oxidation states are summarised in Table 3. Each shows in the [2,2] state a broad region of absorption between 350 and 700 nm with several overlapping transitions; the individual maxima are poorly resolved. These are likely to be the usual $Ru(d_\pi)\rightarrow bipy(\pi^*)$ metal-to-ligand charge-transfer (m.l.c.t.) processes, with a wide spread of energies due to the non-equivalence of the metal d_π orbitals. That the transitions extend to lower energy than in $[Ru(bipy)_3]^{2+}$ is a consequence of the raising of some of the metal d orbitals by the π-donor bridging ligands which will decrease the $Ru(d_\pi)$-to-bipy(π*) separation.[23] The more intense bands in the UV region below 300 nm are characteristic of bipy-based π–π* transitions.

A detailed spectroelectrochemical study of complex **1** was performed by controlled-potential oxidation of the [2,2] species in an optically transparent thin-layer electrode (OTTLE) cell in a variety of solvents (Table 3). To prevent the dissociation of the resulting [2,3] species which occurred at room temperature, the OTTLE cell was cooled to 240 K, and at this temperature the electrochemically generated [2,3] species were indefinitely stable in all of the solvents employed. On oxidation of the [2,2] species to the [2,3] state the m.l.c.t. bands at 589 and 364 nm collapsed and were replaced by new weaker bands at higher energy (Fig. 4) which are also likely to be m.l.c.t. bands. Their shift to higher energy is consistent with the higher charge on the complex which will lower the $Ru(d_\pi)$ levels, but it is not possible to say whether the transitions originate from a localised ruthenium(II) centre perturbed by the nearby positive charge, or from a fully delocalised [2.5,2.5] mixed-valence state.

Table 3 Electronic spectral data for complex **1** in different oxidation states

Oxidation state	λ_{max}/nm (10^{-3} ε/dm^3 mol^{-1} cm^{-1})[a]
[2,2]	572 (12), 420 (sh),[b] 359 (15), 293 (79), 242 (58)
[2,3]	1800 (5), 480 (9), 340 (12), 292 (94), 242 (57)
[3,3]	580 (6), 380 (sh), 248 (64)

[a] Spectra recorded in CH_2Cl_2 at 240 K. [b] sh = Shoulder.

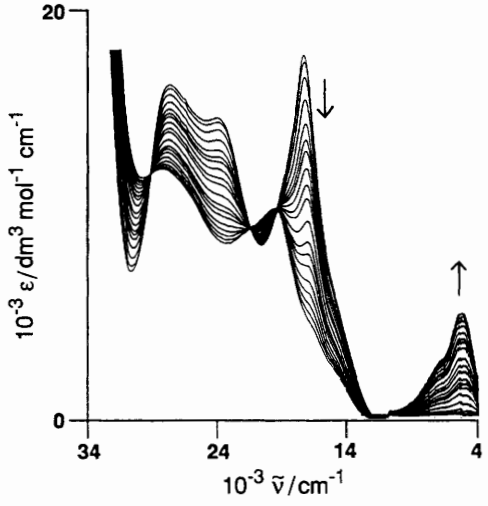

Fig. 4 Successive electronic spectra of complex **1** in propylene carbonate (4-methyl-1,3-dioxalan-2-one) at 240 K recorded during electrochemical oxidation to the mixed-valence $Ru^{II}Ru^{III}$ state, showing the disappearance of the $Ru^{II}\rightarrow$bipy m.l.c.t. bands and the appearance of the near-IR band

The most significant feature of the electronic spectrum of the mixed-valence species is an intense new band at approximately 1750 nm (5700 cm^{-1}) with an absorption coefficient of 5000 dm^3 mol^{-1} cm^{-1}. This band has a shoulder at approximately 1330 nm (7500 cm^{-1}). It can be considered to arise from transitions from bonding electrons in the Ru_2O_2 bridge to the gap in the singly occupied HOMO; considering the spread of orbital energies that was apparent from the ZINDO calculation, it is not surprising that a second component is visible as a shoulder. Measurement of the position of the band maximum in a range of solvents (MeCN, EtCN, PhCN, dimethylformamide, CH_2Cl_2, acetone, pyridine, propylene carbonate) showed that it is not solvatochromic. This is generally characteristic of class III (fully delocalised) mixed-valence species in which the transition is effectively a π–π* transition delocalised over the $Ru_2(\mu\text{-}O)_2$ core, rather than a valence-localised (class II) species in which the vectorial $Ru^{II}\rightarrow Ru^{III}$ intervalence charge-transfer i.v.c.t. band would be expected to show some degree of solvatochromic behaviour.[24,25] However, in some cases genuine i.v.c.t. bands of class II complexes are only weakly (or not at all) solvatochromic—the complex $[\{Ru(NH_3)_5\}_2(\mu\text{-pym})]^{5+}$ (pym = pyrimidine) is a good example,[17,26]—so this property of the mixed-valence complex is not on its own a conclusive indicator of class III behaviour.

The near-IR transition completely disappears on further oxidation of complex **1** to the [3,3] state which confirms that it is only associated with the mixed-valence state. The most significant feature of the spectrum of the [3,3] complex is a band at 580 nm, which is likely to arise from a pyridyl-to-Ru^{III} ligand-to-metal charge-transfer (l.m.c.t.) transition.[2e]

Application of Hush theory to the mixed-valence complexes

Much useful information regarding the properties of the mixed-valence states may be gleaned from the spectra of the [2,3] species using the equations derived by Hush.[25,27] For symmetric systems where the interaction is moderate or weak the electronic coupling element V_{ab} may be determined from equation (1): V_{ab}, $\Delta\tilde{\nu}_{\frac{1}{2}}$ (the half-width of the band) and $\tilde{\nu}_{op}$ (the

$$V_{ab} = (0.0205/r)(\varepsilon_{max}\Delta\tilde{\nu}_{\frac{1}{2}}\tilde{\nu}_{op})^{\frac{1}{2}} \quad (1)$$

optical band maximum) are in cm^{-1}, ε_{max} is the absorption coefficient of the band in $dm^3\ mol^{-1}\ cm^{-1}$, and r is the metal–metal separation in Å. This equation comes from a perturbation treatment of a donor–acceptor charge-transfer system,[27] and does not apply to class III systems in which the excitation is no longer a vectorial charge transfer but a transition between two delocalised levels. In such cases, V_{ab} may be estimated more accurately from equation (2).

$$V_{ab} = \tilde{\nu}_{op}/2 \quad (2)$$

For class II mixed-valence species derived from symmetrical compounds the half-width of the i.v.c.t. band (*i.e.* the width of the signal at half the maximum height) should be related to the energy of the band maximum by equation (3), and this

$$\Delta\tilde{\nu}_{\frac{1}{2}} = (2310\ \tilde{\nu}_{op})^{\frac{1}{2}} \quad (3)$$

relation holds for very many mixed-valence systems.[1] For class III species, however, the half-width of the transition will be substantially less than the value predicted by equation (3) and this is a useful diagnostic test for class III mixed-valence behaviour.[17,25] Using the Creutz–Taube ion, generally considered to be at the lower end of class III behaviour, as an example, equation (3) predicts $\Delta\tilde{\nu}_{\frac{1}{2}} = 3800\ cm^{-1}$ whereas the experimentally determined value is only $1200\ cm^{-1}$.[17b]

From equation (3) the predicted half-width of the near-IR band of complex **1** is $3600\ cm^{-1}$, which is nearly double the actual value of *ca.* $2000\ cm^{-1}$. This is a good indication of class III behaviour. The interaction energy can therefore be estimated from equation (2) to give $V_{ab} = 2800\ cm^{-1}$, a similar value to that of the Creutz–Taube ion. [Note that inappropriate use of equation (1) would give $V_{ab} = 1500\ cm^{-1}$, a significant underestimate.] Together with the large value of K_c derived from the electrochemical data, these results are all consistent with **1** and **2** having a delocalised, class III mixed-valence state. This is also consistent with the nature of the molecular orbital involved which, as was shown earlier, can facilitate delocalisation between the metal centres *via* overlap between the ruthenium d_{xz} orbitals and the oxygen p_x orbitals.

References

1 M. D. Ward, *Chem. Soc. Rev.*, 1995, **24**, 121.
2 For more recent examples of ruthenium-based mixed-valence systems, see (*a*) V. Kasack, W. Kaim, H. Binder, J. Jordanov and E. Roth, *Inorg. Chem.*, 1995, **34**, 1924; (*b*) N. A. Lewis and W. Pan, *Inorg. Chem.*, 1995, **34**, 2244; (*c*) M. Moscherosch, E. Waldhör, H. Binder, W. Kaim and J. Fiedler, *Inorg. Chem.*, 1995, **34**, 4326; (*d*) A. R. Rezvani, C. E. B. Evans and R. J. Crutchley, *Inorg. Chem.*, 1995, **34**, 4600; (*e*) M. D. Ward, *Inorg. Chem.*, 1996, **35**, 1712.
3 Recent examples of mixed-valence systems based on other metals, Y. Maeda, K. Kawano and T. Oniki, *J. Chem. Soc., Dalton Trans.*, 1995, 3533; T.-Y. Dong, S.-H. Lee, C.-K. Chang and K.-J. Lin, *J. Chem. Soc., Chem. Commun.*, 1995, 2453; A. Wlodarczyk, J. P. Maher, J. A. McCleverty and M. D. Ward, *J. Chem. Soc., Chem. Commun.*, 1995, 2397; R. R. Ruminski, D. Serveiss and M. Jacquez, *Inorg. Chem.*, 1995, **34**, 3358; W. Bruns, W. Kaim, E. Waldhör and M. Krejcik, *Inorg. Chem.*, 1995, **34**, 663; Y. Imbe, K. Umakoshi, C. Matsunami and Y. Sasaki, *Inorg. Chem.*, 1995, **34**, 813.
4 D. A. Bardwell, J. C. Jeffery, L. Joulié and M. D. Ward, *J. Chem. Soc., Dalton Trans.*, 1993, 2255.
5 D. A. Bardwell, F. Barigelletti, R. L. Cleary, L. Flamigni, M. Guardigli, J. C. Jeffery and M. D. Ward, *Inorg. Chem.*, 1995, **34**, 2438.
6 S. L. McWhinnie, S. M. Charsley, C. J. Jones, J. A. McCleverty and L. J. Yellowlees, *J. Chem. Soc., Dalton Trans.*, 1993, 413.
7 B. P. Sullivan, D. J. Salmon and T. J. Meyer, *Inorg. Chem.*, 1978, **17**, 3334.
8 SHELXTL 5.03 program system; Siemens Analytical X-Ray Instruments, Madison, WI, 1995.
9 T. R. Weaver, T. J. Meyer, S. A. Adeyemi, G. M. Brown, R. P. Eckberg, W. E. Hatfield, E. C. Johnson, R. W. Murray and D. Untereker, *J. Am. Chem. Soc.*, 1975, **97**, 3039; S. W. Gersten, G. J. Samuels and T. J. Meyer, *J. Am. Chem. Soc.*, 1982, **104**, 4049; F. Bottomley and M. Mukiada, *Inorg. Chim. Acta*, 1985, **97**, L29.
10 E. C. Johnson, B. P. Sullivan, D. J. Salmon, S. A. Adeyemi and T. J. Meyer, *Inorg. Chem.*, 1978, **17**, 2211.
11 J. A. Connor, T. J. Meyer and B. P. Sullivan, *Inorg. Chem.*, 1979, **18**, 1388.
12 Y. Gao, A. Frost-Jensen, M. R. Pressprich, P. Coppens, A. Marquez and M. Dupuis, *J. Am. Chem. Soc.*, 1992, **114**, 9214.
13 B. M. Holligan, J. C. Jeffery, M. K. Norgett, E. Schatz and M. D. Ward, *J. Chem. Soc., Dalton Trans.*, 1992, 3345.
14 D. P. Rillema, D. S. Jones and H. A. Levy, *J. Chem. Soc., Chem. Commun.*, 1979, 849.
15 F. A. Cotton and R. A. Walton, *Multiple Bonds between Metal Atoms*, Oxford University Press, New York, 1993.
16 M. B. Robin and P. Day, *Adv. Inorg. Chem. Radiochem.*, 1967, **10**, 247.
17 (*a*) D. E. Richardson and H. Taube, *Coord. Chem. Rev.*, 1984, **60**, 107; (*b*) C. Creutz and H. Taube, *J. Am. Chem. Soc.*, 1973, **95**, 1086.
18 M. Tanner and A. Ludi, *Inorg. Chem.*, 1981, **20**, 2348; G. M. Tom and H. Taube, *J. Am. Chem. Soc.*, 1975, **97**, 5310.
19 H. Krientzien and H. Taube, *Inorg. Chem.*, 1982, **21**, 4001; S. I. Amer, T. P. Dasgupta and P. M. Henry, *Inorg. Chem.*, 1983, **22**, 1970.
20 S. Joss, H. B. Bürgi and A. Ludi, *Inorg. Chem.*, 1985, **24**, 949.
21 L. O. Spreer, C. B. Allan, D. B. MacQueen, J. W. Otvos and M. Calvin, *J. Am. Chem. Soc.*, 1994, **116**, 2187.
22 D. V. Pinnick and B. Durham, *Inorg. Chem.*, 1984, **23**, 1440.
23 A. Juris, V. Balzani, F. Barigelletti, S. Campagna, P. Belser and A. von Zelewsky, *Coord. Chem. Rev.*, 1988, **84**, 85.
24 J. T. Hupp and T. J. Meyer, *Inorg. Chem.*, 1987, **26**, 2332; R. L. Blackbourn and J. T. Hupp, *J. Phys. Chem.*, 1988, **92**, 2817.
25 C. Creutz, *Prog. Inorg. Chem.*, 1983, **30**, 1.
26 D. E. Richardson and H. Taube, *J. Am. Chem. Soc.*, 1983, **105**, 40.
27 N. S. Hush, *Prog. Inorg. Chem.*, 1967, **8**, 391; *Coord. Chem. Rev.*, 1985, **64**, 135.

Received 12*th February* 1996; *Paper* 6/00989A